

IGBT Junction Temperature Prediction Using a Hybrid GA–LM Optimized BP Neural Network

Yu Zhang ¹², Tadiwa Elisha Nyamasvisva ³

¹ Ph.D., Students, Faculty of Engineering, Science and Technology, Kuala Lumpur University of Science and Technology, Malaysia.

² Associate Professor, College of Engineering Xi'an Jiaotong University, China.

³ Associate Professor, Faculty of Engineering, Science and Technology, Kuala Lumpur University of Science and Technology, Malaysia.

Abstract

Accurate online prediction of junction temperature is essential for ensuring the reliability of insulated-gate bipolar transistors (IGBTs) in power electronic systems. However, reliable temperature estimation remains challenging due to the nonlinear and current-dependent characteristics of temperature-sensitive electrical parameters under practical operating conditions.

To address this issue, a hybrid GA–LM optimized BP neural network is proposed for IGBT junction temperature prediction. In the proposed framework, a genetic algorithm is employed to perform global optimization of network parameters, while the Levenberg–Marquardt algorithm is subsequently introduced for local refinement, thereby improving convergence efficiency and prediction stability. An experimental platform based on saturation voltage measurement is established to extract temperature-sensitive electrical parameters over a wide range of operating currents.

Experimental results show that the proposed model achieves lower prediction errors and reduced error dispersion across both low-current and high-current operating regions compared with conventional BP and GA–BP methods. The maximum mean absolute percentage error and root mean square error are limited to 0.114 and 7.803, respectively.

The proposed approach provides an effective and practical solution for real-time junction temperature monitoring, with potential applications in thermal management and reliability assessment of IGBT-based power electronic converters.

Keywords: Insulated-Gate Bipolar Transistor (IGBT); Temperature-Sensitive Electrical Parameter (TSEP); Junction Temperature Prediction Model; Genetic Algorithm-Levenberg–Marquardt-Back Propagation (GA-LM-BP) Algorithm; Saturation Voltage; Real-time Monitoring

I. INTRODUCTION

Insulated-gate bipolar transistors (IGBTs) are widely employed in motor drives, high-voltage direct current transmission, renewable energy systems, and other power electronic applications [1–2]. Due to their high-power density and complex operating conditions, IGBT modules are prone to thermal stress, and junction temperature has been recognized as a key factor affecting device reliability and lifetime [3–4]. Existing studies have shown that common failure mechanisms, including bond wire fracture, solder layer fatigue, and metallization degradation, are closely related to junction temperature characteristics such as average temperature,

fluctuation amplitude, and peak value [5–7]. Accurate estimation of junction temperature is therefore essential for fault prediction and health monitoring of power electronic systems.

In practical applications, direct measurement of junction temperature is difficult because the semiconductor chip is encapsulated within the module package. Conventional estimation approaches mainly rely on thermal network models, loss-based methods, or temperature-sensitive electrical parameter (TSEP) techniques. Thermal and loss-based models estimate junction temperature through equivalent thermal parameters and power dissipation calculation. However, their accuracy strongly depends on parameter identification and modeling assumptions, which are sensitive to operating conditions and aging effects. TSEP-based methods utilize electrical characteristics such as saturation voltage or on-state resistance to infer junction temperature, providing improved measurement feasibility, yet their nonlinear behavior and strong dependence on operating current limit prediction robustness under dynamic conditions [8–10].

With the development of data-driven techniques, neural-network-based methods have been increasingly applied to junction temperature prediction. Back-propagation (BP) neural networks can capture complex nonlinear relationships between electrical parameters and junction temperature without explicit physical modeling. Despite their modeling capability, conventional BP networks often suffer from slow convergence and sensitivity to initial parameter selection. To improve prediction performance, optimization strategies such as genetic algorithms (GA) have been introduced to enhance global search capability. However, most GA-optimized BP models primarily focus on weight initialization, while issues related to convergence efficiency, prediction stability, and robustness across different current regions remain insufficiently addressed, particularly near the critical current where temperature-sensitive electrical characteristics change significantly.

Despite these advances, existing studies rarely consider the combined requirements of prediction accuracy, convergence efficiency, and robustness across different operating regions. Moreover, the engineering applicability of many proposed methods is constrained by limited consideration of model stability and real-time deployment requirements.

To address these challenges, this study proposes an IGBT junction temperature prediction model based on a hybrid GA–

LM optimized BP neural network. The main contributions of this work are summarized as follows:

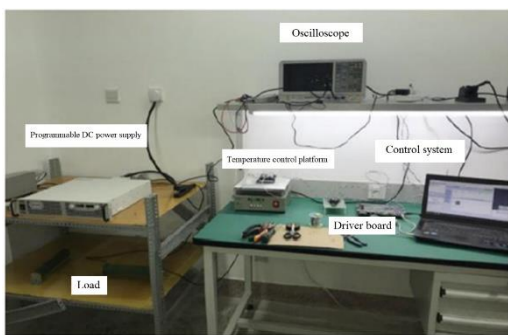
- A hybrid optimization framework combining the global search capability of the genetic algorithm and the fast local convergence of the Levenberg–Marquardt algorithm is employed to enhance training efficiency and prediction accuracy.
- A practical junction temperature prediction model is established using experimentally measured temperature-sensitive electrical parameters, ensuring consistency with real operating conditions.
- The prediction performance of the proposed model is systematically evaluated under different current regions, demonstrating consistent prediction performance across different current regions compared with conventional BP and GA-optimized BP models.
- The proposed method provides a feasible solution for real-time junction temperature estimation, offering practical value for reliability assessment and thermal management in IGBT-based power electronic systems.

II. MODELLING OF JUNCTION TEMPERATURE PREDICTION

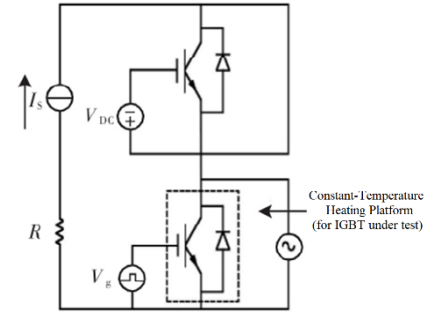
II.I Establishment of the saturation voltage drop experimental platform

This paper takes a 1200V / 75A IGBT module as the research object, and builds a set of saturation voltage drop test platform for the experimental measurement of the saturation voltage drop characteristics of this module. The selected 1200 V / 75 A IGBT module represents a typical medium-power device widely used in industrial motor drives and power conversion systems, making it suitable for investigating junction temperature behavior under practical operating conditions.

The test platform mainly consists of six parts: programmable DC power supply, power load, IGBT driver board, control system, temperature control platform and oscilloscope, and the overall structure is shown in Fig. 1(a), The experimental principle is shown in Fig. 1(b). In this paper, the TSEP method is used to measure the saturation voltage drop without destroying the device package and is easy to operate.



(a) Saturation voltage drop test platform



(b) Saturation Voltage Drop Test Schematic

Fig. 1. Schematic diagram of the IGBT experimental platform

The upper and lower tubes of the half-bridge IGBT module are connected in series, with the upper tube gate applying a negative pressure to ensure reliable shutdown, and the collector shorted to prevent false conduction; the lower tube is used as the measured object for the extraction of junction temperature-related parameters. In order to avoid a blind spot in the measurement of junction temperature T_j by the collector current I_C due to the change of the module's characteristics at high temperatures, the temperature gradient interval is set to be from 25°C to 150°C, and the collector current gradient interval is from 20 A to 200 A.

The selected temperature range covers typical ambient operating conditions as well as elevated junction temperatures approaching the upper thermal limits of commercial IGBT modules, enabling evaluation of model performance under both normal and high-stress thermal states. The current range from 20 A to 200 A spans light-load to high-load operating conditions commonly encountered in power electronic converters, allowing the nonlinear influence of collector current on temperature-sensitive electrical parameters to be sufficiently captured. The experimental conditions, including current range, temperature interval, and single-pulse excitation method, are designed to be consistent with typical operating states of IGBT modules in power electronic converters, thereby enhancing the practical relevance of the obtained dataset. Together, these ranges ensure that the experimental dataset reflects realistic operating scenarios while providing adequate excitation of electro-thermal coupling characteristics for junction temperature prediction.

During the experiment, the thermostat is first set to a specified temperature, and the IGBT module is heated as a whole through the temperature control platform. Continuous heating for a long time, IGBT reached thermal equilibrium, it can be assumed that the chip junction temperature has stabilised at the set value. Subsequently, the IGBT driver board is switched on, the signal generator is triggered with the DC power supply, and a single pulse is used to drive the IGBT to conduct briefly, and the saturation voltage drop V_{CE} is measured simultaneously for this condition, during which the junction temperature T_j , the collector current I_C , the saturation voltage drop V_{CE} , and the enclosure temperature T_c are recorded synchronously. Gradually increase the temperature and repeat the above measurements to obtain the saturation voltage drop and case

temperature data under different junction temperature and collector current conditions.

The three-dimensional surface of the relationship between V_{CE} , I_C and T_j is plotted using the collected data, as shown in Fig. 2. From the Fig. 2, it can be seen intuitively that V_{CE} is affected by I_C and T_j at the same time, which verifies the reasonableness of selecting V_{CE} and I_C as the input parameters of the junction temperature prediction model in this experiment.

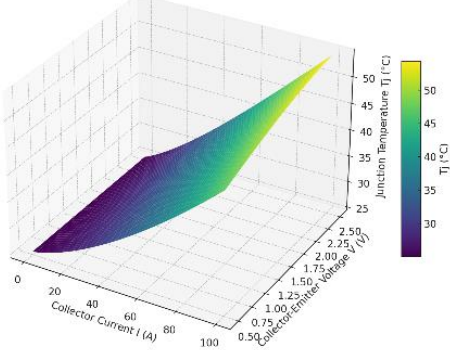


Fig. 2. Three-dimensional diagram of the relationship among V_{CE} , I_C and T_j

II.II BP neural network prediction model

Based on experimental data, it is difficult to clearly define the complex nonlinear relationship between the saturation voltage drop V_{CE} , collector current I_C , case temperature T_C and junction temperature T_j of IGBT. Traditional regression methods are often difficult to achieve high accuracy in such problems, while BP neural network, with its strong fault tolerance, self-learning characteristics and nonlinear mapping function, can construct a junction temperature prediction model without pre-determining the specific mathematical relationship between temperature-sensitive electrical parameters and the junction temperature to achieve an accurate junction temperature estimation.

In this paper, V_{CE} , I_C and T_C are selected as model inputs and junction temperature T_j as output. The learning process of BP neural network consists of two stages: forward propagation of the signal and back propagation of the error. Through the gradient descent method, the weights and thresholds of each layer are continuously adjusted along the error back-propagation path, so that the mean-square error of the network is gradually reduced to a minimum.

In the forward propagation process, the input signals V_{CE} , I_C , and T_C are nonlinearly transformed by the implicit layer and passed to the output layer to obtain the predicted value of the junction temperature, T_{jp} . If there is a deviation between T_{jp} and the true value, T_j , the error back propagation process is initiated, and the error is apportioned layer-by-layer to each neuron, accordingly, adjusting the weights of each layer ω_{ak} ($a = 1, 2, \dots, a$; $k = 1, 2, \dots, k$) and the threshold b_c ($c = 1, 2, \dots, c$), so that the network weights and biases are updated in the direction of the fastest decreasing error, and the output error is finally minimized.

The structure of the BP neural network is shown in Fig. 3, where f_Z ($Z = 0, 1, 2, \dots, z$) denotes the number of neurons in the hidden layer.

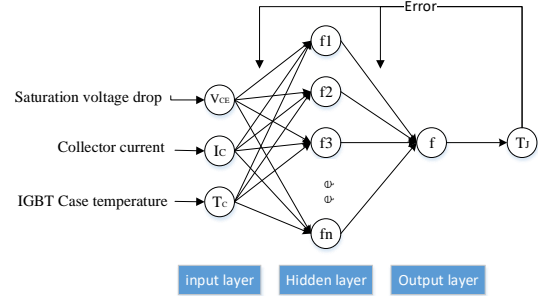


Fig. 3. Structure of the BP neural network algorithm

II.II.I Optimisation of BP model parameters based on genetic algorithm

The junction temperature prediction performance of BP neural network mainly depends on the configuration and cooperation of its weights and thresholds. Although the network is able to automatically extract effective mapping rules by learning the experimental dataset of IGBT junction temperature with real labels, the standard BP algorithm suffers from slow convergence [13]. In general, the predictive ability of the model improves as the degree of training deepens [14], but there exists a critical point for this improvement; beyond this point, the continued enhancement of the training ability will lead to a decrease in the predictive performance, i.e., the phenomenon of "overfitting" occurs.

To overcome this limitation, this paper adopts Genetic Algorithm (GA) to search for the optimal combination of BP neural network weights and thresholds in the global range to construct the GA-BP junction temperature prediction model. This method can significantly improve the regression performance of the model, thus enhancing the stability and accuracy of junction temperature prediction. The flow of the GA-BP neural network algorithm is shown in Fig. 4.

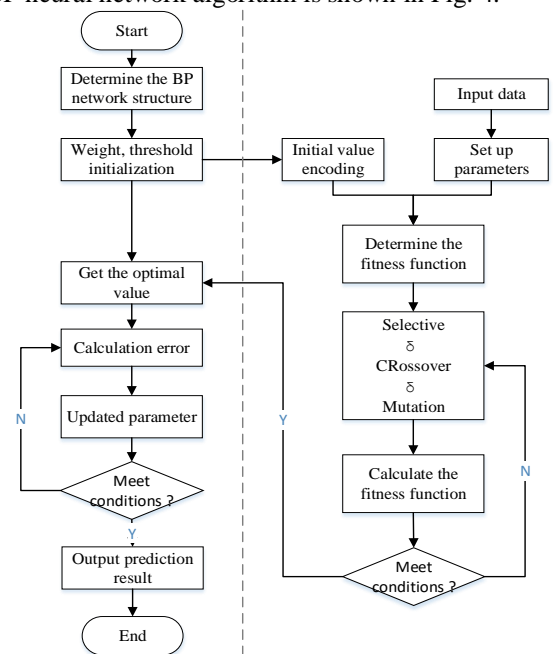


Fig. 4. Flow chart of the GA-BP neural network algorithm

The initial weights and thresholds of the BP neural network are obtained based on the individual, and the system output is predicted after training the BP neural network with the training data, and the sum of the absolute value of the error between the predicted output and the desired output is taken as the individual fitness value F , i.e.

$$F = k(\sum_{i=1}^m |x_i - y_i|) \quad (1)$$

Where: m is the number of junction temperature prediction data; x_i is the i th junction temperature experimental data; y_i is the i th junction temperature prediction data.

II.III.II Optimisation of LM-based BP model parameters

Aiming at the problem that BP neural networks converge slowly and easily fall into the local optimum, this paper proposes a hybrid optimisation strategy combining the global search of the Genetic Algorithm (GA) and the local fine tuning of the Levenberg-Marquardt (LM) algorithm to construct a GA-LM-BP junction temperature prediction model in order to improve the convergence speed and the prediction accuracy at the same time.

Firstly, GA optimisation was used to obtain the initial better solution of the BP neural network weights and thresholds with real number coding, chromosome length of 51, and population size set to 102. The chromosome length is determined by the total number of weights and biases in the BP neural network structure, ensuring complete parameter mapping during genetic encoding. The population size is selected to provide sufficient solution diversity while maintaining acceptable computational complexity for model training.

Individual performance was assessed with a fitness function, and individuals with high fitness were preferentially selected for evolution, and population diversity was maintained through adaptive mutation strategies to avoid precocious maturation.

On this basis, the Levenberg–Marquardt (LM) algorithm is introduced for local fine optimization. The LM algorithm is employed due to its fast convergence characteristics and approximate second-order optimization capability, which are particularly suitable for reducing training time and improving numerical stability in engineering-oriented neural network applications. The network parameters obtained from the Genetic Algorithm (GA) optimization are used as the initial values of the LM algorithm, enabling efficient local refinement following the global search process. During optimization, the mean square error (MSE) of the training set is adopted as the objective function, while the MSE of the validation set is monitored simultaneously to ensure model generalization performance. The error convergence threshold is set to 0.01, which represents a balance between prediction accuracy (within ± 1 °C) and computational efficiency.

This hybrid strategy gives full play to the global exploration capability of GA and the fast local convergence advantage of LM, which significantly improves the model robustness and convergence speed. The flow of the GA-LM-BP neural network algorithm is shown in Fig. 5.

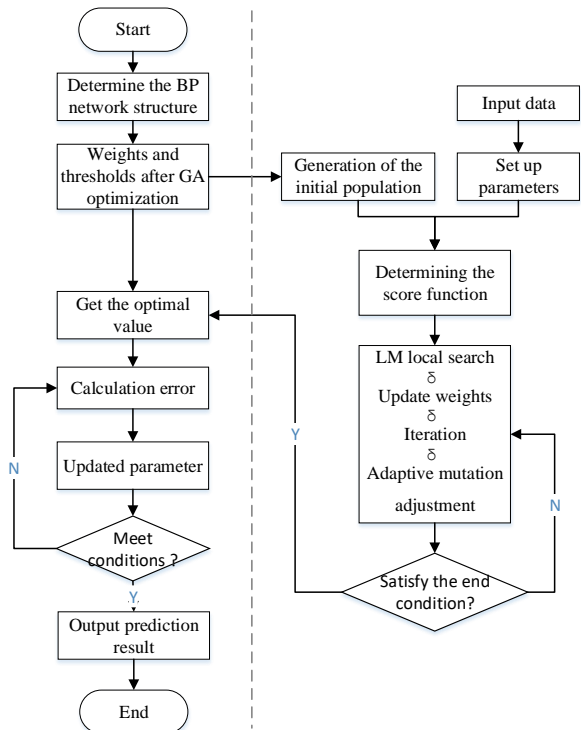


Fig. 5. Flow chart of the GA-LM-BP neural network algorithm

III. EXPERIMENTAL RESULTS

III.I Error metrics

The prediction errors are quantified using the mean absolute percentage error (δ_{MAP}) and the root mean square error (δ_{RMS}), which are calculated as follows:

$$\delta_{MAP} = \frac{1}{m} \sum_{i=1}^m \left| \frac{x_i - y_i}{y_i} \right| \quad (2)$$

$$\delta_{RMS} = \sqrt{\frac{\sum_{i=1}^m (x_i - y_i)^2}{m}} \quad (3)$$

These metrics are used to quantitatively evaluate prediction performance.

III.II Dataset and operating regions

A total of 2250 sets of valid data were obtained from the saturation voltage drop experimental platform. The dataset was divided into training, validation, and test subsets with a ratio of 75%:15%:15%. The parameters of the GA-LM-BP model were set to 102 populations, with 10 winning and 10 temporary subpopulations, and 10 iterations. For comparison, the GA-BP model adopted a population size of 10, a crossover probability of 0.2, and a mutation probability of 0.1.

Fig. 6 presents the relationship between the collector–emitter saturation voltage (V_{CE}) and the junction temperature (T_j) under different collector current (I_C) conditions.

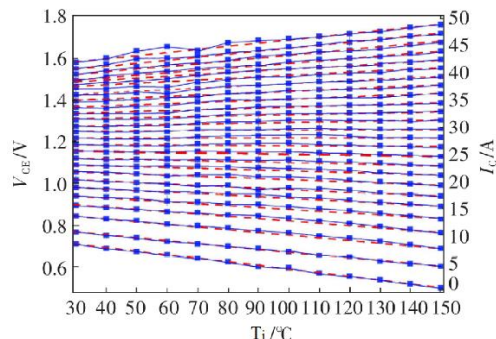


Fig. 6. Relationship between junction temperature and saturation voltage under different collector currents

A transition point around 25 A is observed in the V_{CE} – T_j characteristics. Based on this behavior, the dataset exhibits distinct operating regions separated by a critical current.

III.III Prediction performance comparison

The junction temperature prediction results obtained using the BP, GA–BP, and GA–LM–BP models are summarized in Tables 1 and 2 under low-current ($I_c < 25$ A) and high-current ($I_c > 25$ A) operating conditions, respectively. Differences in prediction results among the three approaches are observed across the investigated operating regions.

Table.1. Experimental and predicted junction temperatures under low-current conditions ($I_c < 25$ A)

I_c /A	V_{CE} /V	T_c /°C	Junction temperature experimental /°C	Junction temperature prediction /°C		
				BP	GA-BP	GA-LM-BP
6.00	0.84	75.2	80.00	83.72	86.91	78.53
6.00	0.88	35.6	40.00	42.63	51.65	44.54
8.00	0.90	74.8	80.00	80.82	86.58	74.86
8.00	0.91	55.3	60.00	67.84	74.25	61.71
10.00	0.95	54.5	60.00	66.38	78.73	61.47
10.00	0.97	34.9	40.00	47.09	58.67	40.72
18.00	1.10	112.6	120.00	110.15	111.51	122.33
18.00	1.11	62.7	70.00	74.32	89.77	73.35
24.00	1.22	61.2	70.00	97.24	97.73	71.38
24.00	1.21	32.4	40.00	103.94	108.24	43.59

Table.2. Experimental and predicted junction temperatures under high-current conditions ($I_c > 25$ A)

I_c /A	V_{CE} /V	T_c /°C	Junction temperature experimental /°C	Junction temperature prediction /°C		
				BP	GA-BP	GA-LM-BP
28.00	1.30	89.1	100.00	134.05	128.15	117.91
28.00	1.27	49.3	60.00	41.37	47.66	55.18
32.00	1.33	37.2	50.00	47.01	42.82	48.77
32.00	1.37	96.8	110.00	109.52	114.59	113.64
40.00	1.48	52.2	70.00	72.78	72.94	70.45
40.00	1.51	91.9	110.00	110.41	109.06	116.93
44.00	1.54	49.7	70.00	70.18	71.37	69.23
44.00	1.49	10.3	30.00	20.75	22.98	29.29
48.00	1.54	7.8	30.00	24.85	14.41	27.79
48.00	1.65	70.7	100.00	97.22	96.23	97.45

Under low-current conditions, variations in absolute prediction error are more evident among the tested samples. The prediction errors produced by the three models exhibit different levels of dispersion, suggesting non-uniform error distributions within this operating region.

When the collector current exceeds the critical value, the overall prediction errors decrease for all three algorithms. The dispersion of prediction results becomes smaller, and the

prediction values exhibit reduced error dispersion across samples.

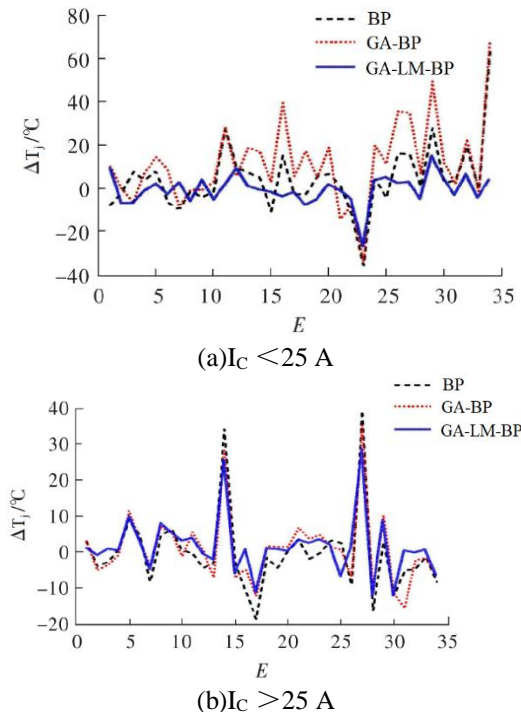


Fig. 7. Absolute junction temperature prediction errors of different algorithms under two current regions

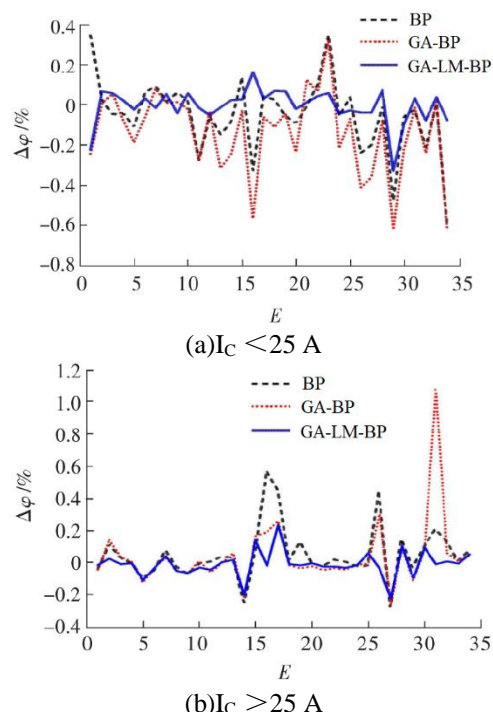


Fig. 8. Relative prediction error distributions of different algorithms under varying current conditions

Prediction error distributions differ between the two current regions, indicating non-uniform prediction behavior under varying operating conditions.

Table 3. Statistical comparison of prediction errors for different algorithms

Algorithm	Working Condition	δ_{RMS}	δ_{MAP}
BP	IC <25A	15.228	0.138
	IC >25A	11.992	0.104
GA-BP	IC <25A	16.624	0.148
	IC >25A	10.026	0.093
GA-LM-BP	IC <25A	13.791	0.114
	IC >25A	7.803	0.062

In addition, the statistical evaluation results listed in Table 3 summarize the corresponding RMSE and MAPE values for the three models under both operating regions, providing a quantitative basis for performance comparison.

IV. DISCUSSION

IV.I Performance difference among algorithms

The prediction performance differences observed among the BP, GA-BP, and GA-LM-BP models mainly arise from their distinct parameter optimization mechanisms. Conventional BP networks rely on gradient-based learning, which makes the training process sensitive to initial weights and susceptible to local optima, particularly when modeling complex electro-thermal nonlinearities.

Genetic algorithm optimization alleviates this limitation by enabling global exploration of the weight-bias search space and reducing dependence on initial parameter selection. However, because GA employs stochastic evolution, its convergence efficiency during later training stages remains limited.

By introducing the Levenberg–Marquardt algorithm after GA optimization, the proposed GA–LM–BP model integrates global search with efficient local refinement. The approximate second-order characteristics of the LM algorithm enable faster convergence and more accurate parameter adjustment. This complementary optimization mechanism explains the lower prediction errors summarized in Table 3 and the error distributions observed in Fig. 7.

IV.II Analysis under different current regions

Distinct prediction behaviors are observed under low-current and high-current operating conditions, which can be attributed to the conduction characteristics of the IGBT module. As shown in Fig. 6, a transition point appears near a collector current of 25 A, separating two operating regions with different temperature-sensitive parameter responses.

Below the critical current, PN-junction conduction dominates and the temperature coefficient of the saturation voltage exhibits strong nonlinearity. Such behavior increases modeling difficulty and leads to larger error dispersion, as reflected in the low-current prediction results in Fig. 7.

When the collector current exceeds the critical value, MOS channel conduction becomes dominant. The relationship between saturation voltage and junction temperature becomes

more regular, resulting in reduced nonlinearity and improved consistency of electro-thermal coupling. Consequently, prediction errors decrease and dispersion is reduced across all models, as reflected in Figs. 7 and 8 and the statistical results in Table 3.

IV.III Comparison with existing studies

Several recent studies have investigated junction temperature prediction of IGBTs using temperature-sensitive electrical parameters and machine learning techniques. For example, neural-network-based models optimized by genetic algorithms have been reported to improve prediction accuracy compared with conventional BP networks [11-12]. Other studies have explored hybrid learning strategies or data-driven approaches to enhance nonlinear modeling capability under specific operating conditions [13].

Compared with these methods, the proposed GA-LM-BP model introduces a two-stage optimization strategy that combines global parameter exploration with efficient local refinement. While existing GA-based approaches primarily focus on improving initial parameter selection, the present work further addresses convergence efficiency and prediction stability by incorporating the Levenberg–Marquardt algorithm. This difference contributes to the reduced prediction error variation observed across operating regions, as summarized in Table 3.

In addition, many previously reported models evaluate prediction accuracy under a single operating condition or within a limited current range. In contrast, this study explicitly analyzes model performance across low-current and high-current regions separated by the critical current, providing deeper insight into robustness under practical load variation.

IV.IV Engineering and industrial application significance

From an engineering perspective, the results of this study provide several practical implications for the application of junction temperature prediction models in power electronic systems.

The observed performance difference between low-current and high-current regions indicates that prediction accuracy is closely related to conduction mechanisms. For practical deployment, this suggests that model validation should cover multiple operating regions rather than relying on data collected at a single current level.

In addition, the reduced error dispersion achieved by the GA-LM-BP model under varying load conditions is beneficial for real-time thermal protection and reliability assessment. Stable prediction behavior enables more reliable threshold setting for temperature-based protection strategies, reducing the risk of false alarms or delayed responses.

Moreover, because the proposed method relies solely on temperature-sensitive electrical parameters without requiring additional temperature sensors or complex thermal modeling, it can be integrated into existing converter control platforms with minimal hardware modification. This characteristic makes the

approach suitable for online junction temperature monitoring in industrial motor drives, renewable energy converters, and electric vehicle power electronics.

These characteristics collectively indicate that the proposed method offers a feasible balance between prediction accuracy, computational efficiency, and implementation complexity for industrial IGBT temperature monitoring applications.

IV. CONCLUSION

This study proposed an IGBT junction temperature prediction method based on a hybrid GA-LM optimized BP neural network and validated its performance using experimentally measured temperature-sensitive electrical parameters. The results demonstrate that the proposed model achieves lower prediction errors and reduced error dispersion across both low-current and high-current operating regions when compared with conventional BP and GA-BP approaches.

The main contribution of this work lies in the integration of global genetic optimization and local Levenberg–Marquardt refinement, which enhances convergence efficiency, prediction stability, and robustness under varying load conditions. In addition, the explicit analysis of prediction behavior across different current regions provides deeper insight into the influence of conduction mechanisms on electro-thermal modeling accuracy.

Despite the improved performance, the present study is limited by the use of experimental data obtained from a single IGBT module under controlled laboratory conditions. The generalization capability of the proposed model across different device types and long-term operating environments has not yet been fully investigated.

Future work will focus on expanding the dataset to include multiple IGBT modules and operating scenarios, as well as exploring real-time implementation and edge deployment strategies for online junction temperature monitoring in practical power electronic systems.

REFERENCES

- [1] Geng Xuefeng, He Yunze, Li Mengchuan, et al. Overview of IGBT multiphysics field modelling techniques and application research[J]. Chinese Journal of Electrical Engineering,2022,42(01):271-290.DOI:10.13334/j.0258-8013.pcsee.210219.
- [2] WANG Weilong, XIANG Liping, ZHAO Guangpan. A review of IGBT power module cooling system applications[J]. Locomotive Electric Drive,2022, (06):130-137.DOI:10.13890/j.issn.1000-128X.2022.06.019.
- [3] Falck J, Felgemacher C, Rojko A, et al. Reliability of Power Electronic Systems: An Industry Perspective [J]. IEEE Industrial Electronics Magazine, 2018.DOI:10.1109/MIE.2018.2825481.
- [4] Dugal F, Ciappa M., Study of thermal cycling and temperature aging on PbSnAg die attach solder joints for high power modules[J]. Microelectronics Reliability,

2014, 54(9-10):18561861. DOI:10.1016/ j.microrel. 2014.08.001.

[5] Kang Y, Dang L, Yang L, et al. Research Progress in Failure Mechanism and Health State Evaluation Index System of Welded IGBT Power Modules[J]. Electronics 2023, 12 (15): 27. DOI:10.3390/electronics12153248.

[6] Zhao S., Yang X., Wu X., et al. Investigation on fatigue mechanism of solder layers in IGBT modules under high temperature gradients [J] Microelectronics Reliability, 2023,141:114901-.DOI:10.1016/j.microrel.2023.114901.

[7] Deng Erping, Liu Peng, Lv Xianliang, et al. Influence of junction temperature conditions on failure modes of IGBT devices in power cycling tests[J]. Semiconductor Technology,2024,49(06):580-588.DOI:10.13290/j.cnki.bdtjs.2024.06.012.

[8] HU Fengye, CUI Haoyang, ZHUO Suohang, et al. Dynamic thermal network model for real-time temperature feedback of IGBT modules[J]. Semiconductor Technology,2020,45(02):138-144.DOI:10.13290/j.cnki.bdtjs.2020.02.008.

[9] Sathik M H M., Jet T K., Kandasamy K., et al. Online junction temperature estimation of IGBT modules for Space Vector Modulation based inverter system[J]. IEEE, 2016.DOI:10.1109/SPEEDAM.2016.7525975.

[10] Baker N, Munk-Nielsen S., Iannuzzo F, et al. IGBT Junction Temperature Measurement via Peak Gate Current[J]. IEEE Transactions on Power Electronics, 2016, 31(5):3784-3793.DOI:10.1109/TPEL.2015.2464714.

[11] Miao J G, Yin Q, Wang H, et al. IGBT junction temperature estimation based on machine learning method[C]/2020 IEEE 9th international power electronics and motion control conference (IPEMC2020-ECCE Asia). IEEE, 2020: 1-5.

[12] Wang H, Xu Z, Ge X, et al. A junction temperature monitoring method for IGBT modules based on turn-off voltage with convolutional neural networks[J]. IEEE Transactions on Power Electronics, 2023, 38(8): 10313-10328.

[13] Du Z W, Zhang Y, Wang Y, et al. A Time Series Characterization of IGBT Junction Temperature Method Based on LSTM Network[J]. IEEE Transactions on Power Electronics, 2024.

FUNDING STATEMENT

This work was supported by the Natural Science Basic Research Program of Shaanxi Province (Grant No. 2024JC-YBQN-0603); Scientific Research Program Funded by Shaanxi Provincial Education Commission (Grant No. 23JK1602); Chancellor's Fund Research Projects by Xian Siyuan University (Grant No. XASYB24ZD02).